Recent Advances in Potentiometric Scanning Electrochemical Microscopy

Thesis booklet

Author:
ANDRÁS KISS
Doctoral School of Chemistry
Department of General and Physical Chemistry

Doctoral Supervisor:
Prof. Dr. GÉZA NAGY
Department of General and Physical Chemistry

Head of Doctoral School:
Prof. Dr. FERENC KILÁR
Department of Analytical and Environmental Chemistry

University of Pécs

April 16, 2017

1 Introduction

Since the invention of Scanning Tunnelling Microscopy (STM) in 1981 by Binnig and Rohrer, surface analysis has seen tremendous growth. The fact that they received the Nobel Prize in 1986, only five years later, is an indication of the importance of their pioneering work. STM was but the first of a family of techniques, called Scanning Probe Microscopy (SPM), with many more to come in the following years. Their basic element is a local experiment, which is repeated sequentially at the pre-defined points of a raster grid. Then, the gathered information is presented by plotting the measured parameter as a function of their coordinate. The most important advantage of them over the conventional optical microscopy is their incredible resolution. Even individual atoms can be „seen", because they are not limited by Abbes' formula. Modifications of the original STM followed quickly. For instance, Atomic Force Microscopy was invented in 1982 by the same researchers.

In 1989, not long after the introduction of the STM, electrochemists invented the Scanning Electrochemical Microscope (SECM), the electrochemical version of SPM. It is based on the same concept, except the scanning probe is a microelectrode. With this technique, highly resolved chemical information can be gathered about a wide range of surfaces. One of the biggest disadvantages of the SPM techniques in general is their low speed, due to the scanning process. The entire image is recorded with the same measuring tip, as opposed to optical techniques, where there is usually a sensor array. As a consequence of this, the more data points are in an image, the longer it will take to record it. This is especially a problem in the potentiometric operation mode of the SECM. The response time of the measuring cell is determined by the RC time constant, which in turn, depends mainly on the resistance of the measuring microelectrode. Due to the small size of the microelectrodes, their resistance can even reach the GΩ range, resulting in imaging times that can be measured in minutes.

Other SPM techniques have received significant improvement during the last few decades, and their imaging speed can even reach video framerates. Low speed, however, is an often overlooked limitation of the SECM, and prevents the quick recording of highly resolved images. That is, one has to choose between high resolution and quick imaging. The image will either be quickly completed but distorted, or high quality but asynchronous, because the points of the image will not only have different spatial, but different temporal coordinates as well.

My thesis is mostly devoted to the investigation of this problem, and three possible solutions to it:

1. Use of novel, low-resistance solid contact electrodes instead of conventional ones.

2. Optimization of scanning patterns and algorithms.

3. Deconvolution of distorted potentiometric SECM images recorded with high scanrate.

The first approach I took is to lower the resistance of the measuring microelectrode. By using a conducting polymer based solid internal contact instead of the conventional liquid contact, electrode resistance, therefore RC time-constant of the entire potentiometric circuit can be decreased. Conducting polymers have been used in macroelectrodes before, but never where it is crucial to have a small resistance despite the small probe diameter: SECM investigation of corroding surfaces.

The second approach is to optimize scanning patterns. Many studied systems have a certain symmetry which can be exploited to achieve lower distortion. I chose a simple, yet very common symmetry, the radial symmetry, and came up with optimized scanning patterns and algorithms.

The third technique is image processing. The relationship between cell potential difference and time is relatively simple, and by measuring some basic parameters of the microelectrode and the potentiometric cell, a deconvolution function can be obtained. With this, the equilibrium potential can be calculated for each data aquisition point of the raster grid, and distortion can be removed from the image.

To investigate the performance of these techniques, I've used simple model systems, then, I've applied them in corrosion studies as an example where they can be useful. During collaborations with colleagues, I used these techniques on several occasions, and I've included some of those results in my thesis.

Additionally, I investigated the undesired effect of electric field generated in certain SECM experiments. In some cases, where there is a potential difference between two points in the electrolyte, a relatively strong electric field can be formed. For instance during galvanic corrosion there is a large potential difference between the surfaces of the metals constituting the galvanic couple. The local electric field at the tip of the measuring electrode might influence the measured potential. I investigated this contribution to the measured value, and tried to isolate the effect of the electric field.

2 Methods

Most of the measurements in my dissertation are high impedance potential measurements. Impedance matching was either provided by the instrument or by a home made TL082 operational amplifier based voltage follower circuit. This was needed

to avoid loading error present in measuring high impedance voltage sources, such as potentiometric cells employing ion selective microelectrodes.

The SECM instrument and the software controlling its movement was home made. All the ion selective microelectrodes were home made. I have used several different kind of microelectrodes:

- Antimony pH sensitive microelectrodes.
- Tungsten pH sensitive microelectrodes.
- Magnesium ion selective micropipettes.
- Potassium ion selective micropipettes.

Potential was always measured against an Ag/AgCl/(3 M) reference half cell. The deconvolutions and the diffusion/SECM simulations were performed by a program written in FORTRAN.

3 Results and Discussion

3.1 Using solid-contact microelectrodes as potentiometric SECM probes

Solid-contact electrodes have lower resistance, compared to their otherwise identical, liquid-contact counterparts. This is due to two reasons. The solid contact can be pushed down very close to the micropipette orifice, shortening the thickness of the highly resistive ion-selective membrane, and decreasing the overall electrode resistance. The other reason is that instead of the internal solution – which has high resistance –, a modified carbon fiber – which has low resistance – is used as the ion-to-electron transducer. If R is lower, RC is lower, and the potentiometric cell becomes faster.

I constructed two Mg^{2+}-ion selective electrodes. One used a liquid contact, and the other a solid contact. Besides this difference, they were prepared identically. Basic characterisation was performed for both. Response characteristics were investigated by measuring the electrode resistance R, and the τ_{95} response time. Calculated from the voltage divider measurements, electrode resistance was 4.8 GΩ and 0.56 GΩ for the liquid, and solid contact electrodes, respectively. Based on these values, the solid contact electrode was expected to produce less distorted images with the same scanning parameters.

To confirm it, a Mg^{2+} ion diffusion source model system was created, and the plane 100 µm above the pipette orifice was scanned with both electrodes. Fig. 1

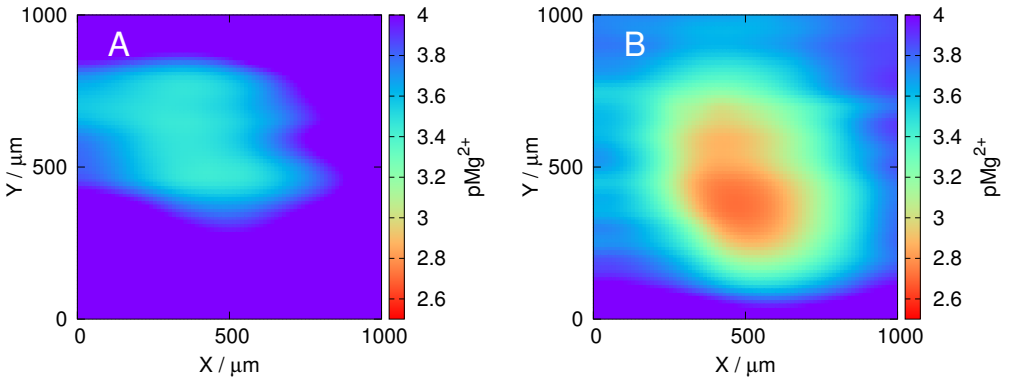

Figure 1: SECM images displaying the Mg^{2+} ion concentrations 100 µm above the tip of a centered pipette source. (A) liquid-contact, and (B) solid-contact. Scan rate: 12.5 µm/s.

shows the ISME images obtained using a liquid-contact (A), and a solid-contact (B), micropipette electrode. Both 2D ISME maps were recorded at the same scan rate. An upside down glass micropipette holding the 0.1 M $MgCl_2$ agar solution was used in the measurements plotted in Figs. 1A and 1B. Visual inspection of the two images clearly shows significant image distortion in the X-direction with the liquid-contact ISME due its slower response as expected based on its higher resistance. It can also be observed in the image scanned with the solid-contact electrode, although to a much less extent. Another important feature to note in the images is the difference in the highest magnesium ion concentration observed with the two electrodes. With the solid-contact microelectrode it's about $10^{-2.5}$ M. On the other hand, with the conventional liquid-contact electrode, highest observed magnesium ion concentration is only about $10^{-3.4}$ M. One possible reason for this is that the cell equipped with the liquid-contact electrode cannot keep up with the changes of the magnesium ion concentration at the micropipette orifice.

One application that is included in my dissertation is the investigation of the galvanic corrosion of magnesium and its alloys. A solid contact magnesium ISME was used to map magnesium ion distribution above a corroding AZ63 magnesium-aluminium alloy. Vertical Mg^{2+} ion concentration distribution was determined at different instants in time of the corrosion process, with, and without coupling the Mg/Al and Fe samples. Using the Mg^{2+} concentration profiles, Mg^{2+} flow rate from the Mg piece was possible to estimate:

$$\Omega = 4DC_s a \tag{1}$$

where Ω is the amount of Mg^{2+} released from the disc shaped Mg/Al surface, D is the diffusion coefficient of Mg^{2+}, C_s is the surface concentration of Mg^{2+} (at

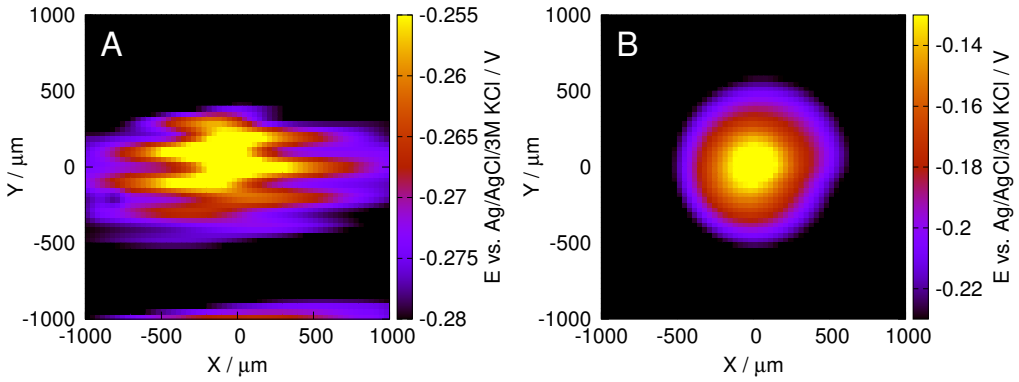

Figure 2: Experimental SECM scans 100 µm above the disc source with the (A) meander and the (B) arc scanning algorithms. Measuring electrode was a pH-sensitive antimony micro-electrode.

the height $z = 0$ µm), a is the radius of the Mg/Al sample. As the only unknown variable in the equation above, Ω could be calculated.

Corrosion current between the Mg/Al sample and the Fe sample was also measured directly. Using Faraday's law of electrolysis, corrosion current could be calculated, and it was in fairly good agreement with the SECM measurement.

3.2 Optimization of scanning algorithms

In the second and third approaches I exploit the properties of the potentiometric response function:

$$E_{cell}(t_e) = E_{cell}(\infty) + [E_{cell}(0) - E_{cell}(\infty)]e^{-t_e/RC} \tag{2}$$

where $E_{cell}(t)$ is the cell potential difference at time t_e, $E_{cell}(\infty)$ is the equilibrium cell potential difference, $E_{cell}(0)$ is the cell potential difference prior to the change. The more different $E_{cell}(0)$ and $E_{cell}(\infty)$ are, the more the difference between $E_{cell}(\infty)$ and $E_{cell}(t_e)$ will be. Distortion of an image can be measured as an average of the differences between $E_{cell}(\infty)$ and $E_{cell}(t_e)$ at each point. It can be lowered by carefully optimizing scanning patterns and algorithms, so that the probe passes through borders between regions of high and low concentrations as few times as possible.

The results (Figure 2) confirmed the presumption, that using the two new algorithms, images have less distortion, with higher similarity to the expected image.

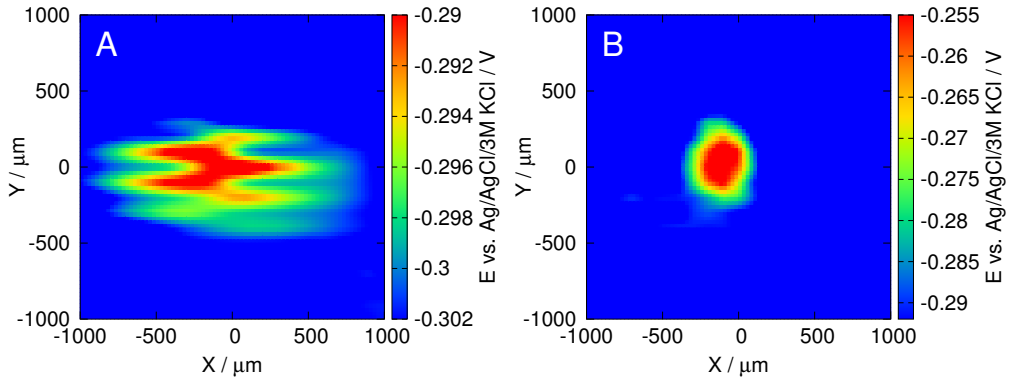

Figure 3: SECM pH image before (A) and after (B) deconvolution. Scan conducted with the antimony microelectrode. Note the different potential scales. Deconvolution restores not only the shape of the concentration profile, but the magnitude of the peak as well. The raster scan pattern was used with the meander algorithm starting in the bottom left corner of the image.

3.3 Signal processing in potentiometric SECM

In the third approach, I use the inverse of the potentiometric response function (Eq. 2) as deconvolution function. Since the relationship between t_e, $E_{cell}(0)$, $E_{cell}(t_e)$ and $E_{cell}(\infty)$ is known, a prediction for the only unknown $E_{cell}(\infty)$ can be calculated.

2D SECM scan was performed above a circular graphite anode (Fig. 3A), with the meander scanning algorithm. Line blur distortion in the raw images is visible along the alternating scanlines used by the meander scanning algorithm. By deconvoluting the image, the expected potential map can be obtained (Fig. 3B).

Not only the circular shape of the target in the images is restored, but the peak value above the center of the target as well. Maximum value in the raw scans was around -300 mV, whereas in the deconvoluted image, it was about -260 mV, with a significant difference between the two.

I obtained similar results with ionophore based ion selective micropipettes, which can be found in my dissertation. I haven't included those results here, due to the compact format of this booklet.

As an example of the application of the technique, corroding carbon steel was imaged. As expected, the image was distorted, and without any processing evaluation proved to be difficult. The irregular shape of the target was recognisable after, but not before the deconvolution. The difference between the original and the processed image was quite large. Without any processing, pH would have been misestimated by about 1 pH unit. A different conclusion can be drawn based on the raw, and the deconvoluted image.

Another studied technique was blind deconvolution. This is the technique of de-

convoluting measured data without the complete knowledge of the transfer function that describes the convolution. To explore this possibility, I deconvoluted a pH image using the deconvolution function with several different time-constant substituations, including the measured one.

The best result could be easily recognized just by visual inspection, and it was the one that was deconvoluted by the correct, measured time-constant. A more advanced method would be a statistical approach, where one would try to detect any correlation between the scanning algorithm – taking into account the scan direction – and the image, and choose the deconvoluted image with the least correlation.

3.4 The effect of electric field on potentiometric SECM images

During galvanic corrosion, ions are being released from the anode. The measured potential of an ion selective microelectrode is thought to depend only on the activity of the primary ion. However, an electric field is also formed as a result of the potential difference between the surfaces of the galvanic pair, which has a direct influence on the potential of the measuring microelectrode. The measured potential is the sum of these two contributions:

$$\Delta E = E_M - E_R + (\phi_M - \phi_R) \tag{3}$$

where ΔE is the measured potential difference, E_M and E_R is the potential of the measuring and the reference electrode, and ϕ_M and ϕ_R are the local potentials in the electric field at the measuring and reference electrodes, respectively.

There are multiple papers featuring contradictory results obtained by studying system where a strong electric field is present. These contradictory results can be explained by a contribution of the electric field that is formed during these experiments.

The ISME was maintained at a constant height from the metal surface, and its potential was recorded as a function of time, while the galvanic connection was established between the two metals (Fig. 4). Thus, the tip was first positioned 100 µm above the center of the AZ63 wire (red curve in Fig. 4), and for about 300 s the spontaneous corrosion of the alloy sample was recorded. Then, the galvanic connection was established, and a sharp increase in potential of about 70 mV could be observed. This change would correspond to a two orders of magnitude increase of Mg^{2+} activity in a very short period of time. When the galvanic connection was removed, a potential change of the same magnitude, though opposite direction could be observed. In order to discard the possibility that this rise could be still explained by an abrupt release of Mg^{2+} from the surface, the experiment was repeated while

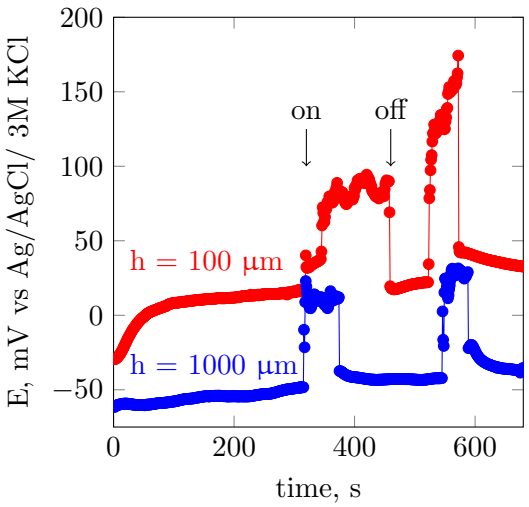

Figure 4: Stationary recordings above the center of the AZ63 target with the ISME placed at: red = 100 µm, blue = 1000 µm distance from the metal. On/off denote the moment when galvanic coupling was either established or ceased. Temporal resolution was 1 Hz.

the tip was positioned 1000 µm above the target (blue curve in Fig. 4). A very similar sequence of potential changes could be observed, despite the big separation between the probe and the corroding sample. The only plausible explanation is that the abrupt change in the recorded potential is due to the electric field developed between the two metals.

The effect of the electric field in certain potentiometric SECM experiments has been demonstrated experimentally, as suspected by certain researchers in corrosion science for some time. A strong electric field is formed around galvanic coupling of dissimilar metals, that causes significant over- or underestimations of the real primary ion activity. The reason for this feature is that the electric field has a direct influence on the measured potential at the ISME.

4 Conclusions

The present work has been devoted to improve potentiometric Scanning Electrochemical Microscopy. Scanning is relatively slow due to the long response time of the potentiometric measuring cell. Shortened scanning time is useful when the studied system is changing. When scanned too fast however, distortion is added to the image. I've successfully sped up the technique without compromising image quality. In another effort, I've managed to separate the effect of electric field from the Nernstian potential response of the ion selective microelectrode.

The main results are summarized in the thesis points:

1. I've successfully shortened response time of the potentiometric cell by using low resistance, solid-contact microelectrodes. I've compared them to conventional, liquid contact microelectrodes by basic characterization and model system study to prove the improved performance.

2. Taking adventage of the new solid-contact electrodes, I've studied the galvanic corrosion of magnesium and the AZ63 magnesium alloy by mapping the concentration of dissolving ions. I used the new solid contact ion selective microelectrodes as SECM probes. This allowed faster scan rates.

3. I've estimated the corrosion current based on the SECM measurements, and compared the result with that obtained with another, established method; the indirect measurement of corrosion current. After applying Faraday's Law of Electrolysis, the two results could be compared. They were very similar, suggesting the applicability of SECM in obtaining quantitative results.

4. I've designed new scanning patterns and algorithms, optimized to radially symmetric targets. I've proven that with these new patterns and algorithms, image distortion is lower compared to the conventional ones, by numerical simulations and experimental SECM scans.

5. I've shown that by using deconvolution, RC distortion can be significantly lowered in the potentiometric SECM images. To prove the validity of the technique, I've compared deconvoluted images to equilibrium images scanned at a rate which allowed to record equilibrium potentials.

6. I've used deconvolution to restore potentiometric SECM images about a corroding carbon steel sample. Evaluation of this data was possible, because scanning time *and* distortion was reduced at the same time.

7. I've shown the applicability of blind deconvolution. This method can be used on measurements where the convolution function cannot be determined.

8. I've proven that the electric field present in many studied systems – galvanically corroding ones in particular – affects the measured potential. The electric field has a direct influence on the measured potential, which is then a sum of this contribution and the Nernstian response associated with ion activity. This effect can cause serious errors in interpretations in the measurements. In this case, the error was almost four orders of magnitude. By taking this effect into account, a more accurate conclusion can be drawn.

5 Publications

5.1 Peer-reviewed publications related to the dissertation

1. Ricardo M. Souto, **András Kiss**, Javier Izquierdo, Lívia Nagy, István Bitter, Géza Nagy, Spatially-resolved imaging of concentration distributions on corroding magnesium-based materials exposed to aqueous environments by SECM, *Electrochemistry Communications 26 (2013): 25-28.*, IF.: 4.85, cited by: 31

2. **András Kiss**, Ricardo M. Souto, Géza Nagy, Investigation of Mg/Al alloy sacrificial anode corrosion with Scanning Electrochemical Microscopy, *Periodica Polytechnica Chemical Engineering 57, no. 1-2 (2013): 11-14.*, IF.: 0.30, cited by: 5

3. Javier Izquierdo, **András Kiss**, Juan José Santana, Lívia Nagy, István Bitter, Hugh S. Isaacs, Géza Nagy, Ricardo M. Souto, Development of Mg^{2+} ion-selective microelectrodes for potentiometric scanning electrochemical microscopy monitoring of galvanic corrosion processes, *Journal of The Electrochemical Society 160, no. 9 (2013): C451-C459.*, IF.: 3.27, cited by: 23

4. **András Kiss**, Géza Nagy, New SECM scanning algorithms for improved potentiometric imaging of circularly symmetric targets, *Electrochimica Acta 119 (2014): 169-174.*, IF.: 4.50, cited by: 8

5. **András Kiss**, Géza Nagy, Deconvolution of potentiometric SECM images recorded with high scan rate, *Electrochimica Acta 163 (2015): 303-309.*, IF.: 4.50, cited by: 7

6. **András Kiss**, Géza Nagy, Deconvolution in potentiometric SECM, *Electroanalysis 27, no. 3 (2015): 587-590.*, IF.: 2.14, cited by: 2

7. **András Kiss**, Dániel Filotás, Ricardo M Souto, Géza Nagy, The effect of electric field on potentiometric Scanning Electrochemical Microscopic imaging, *Electrochemistry Communications 77 (2017): 138-141.*, IF.: 4.569

5.2 Presentations and posters related to the dissertation

1. Investigation of Mg/Al alloy sacrificial anode corrosion with Scanning Electrochemical Microscopy, Poster, *Chemical Engineering Workshop '12, Veszprém, 2012.*

2. Investigation of galvanic corrosion of the Fe-Mg galvanic pair with Scanning Electrochemical Microscope, Poster, *Chemical Sensors Workshop '12, Pécs, 2012.*

3. Fabrication of a new, solid contact Mg^{2+} ion-selective electrode, and its application in Scanning Electrochemical Microscopic corrosion studies, Presenttion, *1st Doctoral Workshop on Natural Sciences, Pécs, 2012.*

4. A new, solid contact Mg^{2+} ion-selective electrode as measuring tip for Scanning Electrochemical Microscope in corrosion studies, Presentation, *János Szentágothai Memorial Conference and Student Competition, Pécs, 2012 October 29-30.*

5. New insights in the corrosion mechanism of magnesium by SECM, Presentation, *7th Workshop on Scanning Electrochemical Microscopy (SECM) and Related Techniques, Ein Gedi, Israel, February 17-21, 2013.*

6. High-speed potentiometric SECM imaging of radially symmetric targets, Presentation, *ESEAC Malmö, Sweden, 11-14 June 2013.*

7. Deconvolution of potentiometric SECM images recorded with high scanrate, Poster, *Mátrafüred Conference 2014 Június 13-16, Visegrád, Hungary.*

8. High-speed SECM imaging, Plenar presentation, *Analytica Conference 2016 May 10-13, München, Germany.*

5.3 Peer-reviewed publications unrelated to the dissertation

1. **András Kiss**, László Kiss, Barna Kovács, Géza Nagy, Air Gap Microcell for Scanning Electrochemical Microscopic Imaging of Carbon Dioxide Output. Model Calculation and Gas Phase SECM Measurements for Estimation of Carbon Dioxide Producing Activity of Microbial Sources, *Electroanalysis 23, no. 10 (2011): 2320-2326.*, IF.: 2.14, cited by: 3

2. Ricardo M. Souto, Javier Izquierdo, Juan José Santana, **András Kiss**, Lívia Nagy, Géza Nagy. Progress in scanning electrochemical microscopy by coupling potentiometric and amperometric measurement modes, *Current Microscopy Contributions to Advances in Science and Technology, Formatex Research Center, Badajoz (2012): 1407-1415*, cited by: 3

3. Lívia Nagy, Gergely Gyetvai, **András Kiss**, Ricardo Souto, Javier Izquierdo, Géza Nagy, Speciális célra szolgáló mikroelektródok kifejlesztése és alkalmazása, *Magyar Kémiai Folyóirat 119, 2-3. (2013): 104-109.*

4. Zsuzsanna Őri, **András Kiss**, Anton Alexandru Ciucu, Constantin Mihailciuc, Cristian Dragos Stefanescu, Lívia Nagy, Géza Nagy, Sensitivity enhancement of a „bananatrode" biosensor for dopamine based on SECM studies inside its reaction layer, *Sensors and Actuators B: Chemical 190 (2014): 149-156.*, IF.: 4.10, cited by: 4

5. Javier Izquierdo, Bibiana M Fernández-Pérez, Dániel Filotás, Zsuzsanna Őri, **András Kiss**, Romen T Martín-Gómez, Lívia Nagy, Géza Nagy, Ricardo M Souto, Imaging of Concentration Distributions and Hydrogen Evolution on Corroding Magnesium Exposed to Aqueous Environments Using Scanning Electrochemical Microscopy, *Electroanalysis 28, (2016): 2354-2366.*, IF.: 2.471, cited by: 2

6. A. El Jaouhari, Dániel Filotás, **András Kiss**, M. Laabd, E. A. Bazzaoui, Lívia Nagy, Géza Nagy, A. Albourine, J. I. Martins, R. Wang, SECM investigation of electrochemically synthesized polypyrrole from aqueous medium, *Journal of Applied Electrochemistry 46 (2016): 1199-1209.*, IF.: 2.223

5.4 Presentations and posters unrelated to the dissertation

1. CO_2 Partial Pressure Imaging in Gas Phase with Scanning Electrochemical Microscopy (SECM), Poster, *X. CECE Conference, Pécs, 2010.*

2. Selective Amperometric Determination Of Pyrocatechol and Phenol in Wines with Flow-Injection Analysis, Poster, *X. CECE Conference, Pécs, 2010.*

3. Four-Channel Enzyme Biosensor for Determination of Phenols in Wine, Poster, *X. CECE Conference, Pécs, 2010.*

4. Development of a CO_2 microcell, and its application as measuring tip in Scanning Electrochemical Microscope. Scanning in gas phase over biological samples, Presentation, *XXXIV. Szegedi Kémiai Előadói Napok, Szeged, 2011.*